

MODAL ANALYSIS OF THE FGM BEAM-LIKE STRUCTURES WITH EFFECT OF THE THERMAL AXIAL FORCE

JUSTÍN MURÍN^{*}, MEHDI AMINBAGHAI[†], JURAJ HRABOVSKÝ^{*},
VLADIMÍR KUTIŠ^{*}, JURAJ PAULECH^{*}

^{*}Department of Applied Mechanics and Mechatronics of IPAE, Faculty of Electrical Engineering and Information Technology, Slovak University of Technology in Bratislava, Ilkovičova 3, 812 19 Bratislava, Slovakia
e-mail: justin.murin@stuba.sk, juraj.hrabovsky@stuba.sk, vladimir.kutis@stuba.sk, juraj.paulech@stuba.sk
web page: <http://aladin.elf.stuba.sk/Katedry/KMECH/>

[†]Institute for Mechanics of Materials and Structures, Vienna University of Technology, Karlsplatz 13, A-1040 Vienna, Austria
e-mail: mehdi.aminbaghai@tuwien.ac.at

Key words: FGM beam finite element, Coupled multiphysics problems, Modal analysis, FGM actuator.

Abstract. The modal analysis of the FGM beam-like actuator is presented, where effects of the thermal axial force and the shear force are considered. The temperature load is assumed to be lower as the critical buckling temperature. The longitudinal variation of material properties has been assumed which can be caused by the varying constituent's volume fraction and the temperature dependence of the constituent's material properties. Our new FGM beam finite element has been used in the proposed analysis. An influence of the material properties variation and the thermal axial forces on the actuator eigenfrequency and eigenform has been studied and discussed.

1 INTRODUCTION

Mechatronic systems represent complex integrated intelligent systems making use of a synergy between information technology, electronics, mechanics, communication and control. Mechatronic is one of the most dominant research and application areas in nowadays' engineering, consumer electronics and services. For an optimal utilization of their enormous potential it is necessary to examine, analyze, model, control and optimize their structure and parameters for a wide range of applications. Development of dominant mechatronic parts like sensors and actuators still continues and is strongly dependant on the design of new materials and applications of modern approaches from the information, communication and control technologies.

Mechatronic systems work in the multi-physical domains. Based on the types of interaction they are divided into thermal-mechanical, electro-thermal, electro-magneto-mechanical, piezoelectric and fluid-structural systems. The modelling and control of these complex

systems requires a continuous research and development of new and effective numerical techniques. The most widely used numerical methods in this area are the finite element method (FEM), finite volume method (FVM) and meshless methods. Besides the multi-physical domain character, progress in material engineering also plays a crucial role in the mechatronic systems design. It is, in particular, the ability to precisely define local material properties - functionally graded material (FGM) or change properties according to a controlling parameter (usually temperature) - shape memory alloys (SMA). However, the most important part in the mechatronic system design is their modelling and simulation.

The variation of FGM's material properties can be achieved via a controlled uneven mixing of two or more components e.g. using powder metallurgy, plasma spray applications, etc. or by a change of components' material properties through temperature. Such a material has much better efficiency than its components. Problems that occur at layer-interfaces of classical multi-layer composites are circumventing [1-3]. For these reasons it is of great interest to implement such new materials in the design of mechatronic parts, especially in the case of small dimensions where it is impossible to change mechanical and other physical attributes through a change in cross-section or complicated geometry (elastic joints, stiffness and dynamics properties etc.). A more intelligent and sophisticated function is reached with the implementation of composites made of FGMs. It is inevitable to create new advanced models and finite elements for their precise and effective multiphysical analyses [4], [7]. A number of international and domestic conference contributions emphasize this necessity [8], [9], [10].

Many papers dealing with modal analysis of single FGM beams can be found in literature, e.g. [11], [12], [13]. Mostly transversal variation of material properties has been considered. In papers [14], [15], spatial variation of material properties has been assumed. In [16], new 2D beam finite element has been established, which can be used in modal analysis of the beams made of FGM with transversal and longitudinal variation of macroscopic material properties. Effects of the internal axial force, shear force and elastic foundation have been taken into account.

In the contribution, which is an extension of the work [16], the new beam finite element will be used in modal analysis of the actuator which is built of FGM beams with longitudinal variation of material properties. The effects of the material properties variation and thermal axial force on the eigenfrequency and eigenform will be studied.

2 DESCRIPTION OF THE 2D FGM BEAM FINITE ELEMENT

This chapter is focused on description of the 2D FGM beam finite element, which is based on differential FGM beam equations of transversal and axial vibration. All quantities in following equations are the polynomial functions of x . Homogenization process of the varying material properties and the calculation of other effective finite element parameters is fully described in [14].

2.1 Transversal free vibration

The main equations of the 2nd order beam theory containing the inertia effects (according to the Figure 1) are:

$$R' = -q + kw - \mu\omega^2 w \tag{1}$$

$$M' = Q + m + \bar{\mu}\omega^2 \varphi \tag{2}$$

$$\varphi' = -\frac{M}{EI} - \kappa^e \Rightarrow M = -EI\varphi' - EI\kappa^e \tag{3}$$

$$w' = \varphi + \frac{Q}{G\tilde{A}} \Rightarrow Q = G\tilde{A}w' - G\tilde{A}\varphi \tag{4}$$

Eqs. (1) and (2) present the equilibrium equations for bending in the deformed configuration. Eqs. (3) and (4) are the constitutive relations of the 2nd order beam theory.

Here q is the distributed transversal load ; m is the distributed bending moment; κ^e denotes any applied beam curvature and k is the modulus of elastic Winkler foundation. Further, $\mu = \rho A = \rho_L^H(x)A$ denotes the mass distribution; $\bar{\mu} = \rho I = \rho_L^H(x)I$ is the mass inertial moment distribution, where $\rho_L^H(x)$ is the homogenized mass density distribution. ω is the natural eigenfrequency; R is the transversal force; Q is the shear force; M is the bending moment. The angle of cross-section rotation is φ ; w is the beam's transverse displacement; $B = EI = E_L^{MH}(x)I$ is the homogenized bending stiffness and $G\tilde{A} = G_L^H(x)k^s(x)A$ is the reduced homogenized shear stiffness. I is the moment of inertia, A is the cross-section area, $E_L^{MH}(x)$, $E_L^{NH}(x)$ and $G_L^H(x)$ is the homogenized elasticity modulus for bending, axial and shear loading, respectively. The calculation of the shear correction function $k^s(x)$ is presented in [15]. The first derivative with respect to x is denoted by superscript (').

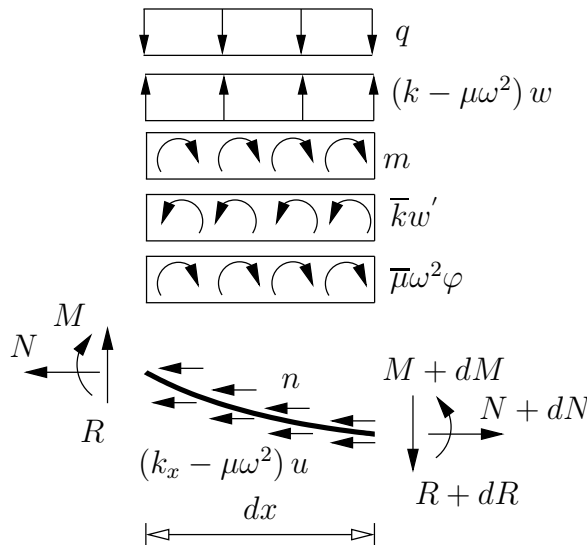


Figure 1: The force equilibrium in the deformed element configuration

The relation between the transversal R and shear Q force is:

$$Q = -(\bar{k} + N^H)w' - N^H\psi + R \tag{5}$$

where $N^H \equiv N$ is the resultant axial force of the 2nd order beam theory (it has to be known and is caused by thermal loads in our case), ψ is the beam rotation imperfection, and $\bar{k} = \bar{k}(x)$ is the elastic foundation modulus for the beam rotation.

Setting the expression (5) into the equations (1) – (4) we get:

$$(\mu\omega^2 - k)w + R' = -q \tag{6}$$

$$G\tilde{A}w' + (\bar{\mu}\omega^2 - G\tilde{A})\varphi - M' = -m \tag{7}$$

$$EI\varphi' + M = -EI\kappa^e \tag{8}$$

$$(\bar{k} + N^H + G\tilde{A})w' - G\tilde{A}\varphi - R = -N^H\psi \tag{9}$$

We get four coupled differential equations which can be solved (after common boundary conditions consideration) for the transfer functions: $w = w(x)$, $\varphi = \varphi(x)$, $M = M(x)$ and $R = R(x)$.

In the modal transversal vibration analysis the right side of the equations (6) – (9) is equal to zero. In the finite element derivation the reduced shear stiffness was simplified: $G\tilde{A} \cong G\bar{A} = G_L^H(x)k^{sm}A$, where instead the shear correction function $k^s(x)$ [15] its average value $k^{sm} = \frac{1}{L} \int_0^L k^s(x)dx$ have been applied (calculation of the average shear correction factor is described in [15]);

After some mathematical operations only one homogeneous differential equation of the 4th order of the homogenized FGM beam deflection with non-constant coefficients has been obtained

$$\eta_4 w'''' + \eta_3 w''' + \eta_2 w'' + \eta_1 w' + \eta_0 w = 0 \tag{10}$$

The non-constant coefficients η_0 to η_4 and appropriated parameters of the differential equation (10) are described in [14] in detail.

If the variation of all beam parameters is polynomial, the solution of this differential equation has a form [17]

$$\begin{bmatrix} w(x) \\ w'(x) \\ w''(x) \\ w'''(x) \end{bmatrix} = \begin{bmatrix} b_0 & b_1 & b_2 & b_3 \\ b'_0 & b'_1 & b'_2 & b'_3 \\ b''_0 & b''_1 & b''_2 & b''_3 \\ b'''_0 & b'''_1 & b'''_2 & b'''_3 \end{bmatrix} \cdot \begin{bmatrix} w_i \\ w'_i \\ w''_i \\ w'''_i \end{bmatrix} \tag{11}$$

where functions b_j , b'_j , b''_j and b'''_j , ($j \in \langle 0,3 \rangle$) are the solution functions of the differential equation (10) and are called transfer functions. The dependence of the $w' = w'(x)$, $w'' = w''(x)$ and $w''' = w'''(x)$ on the $\varphi = \varphi(x)$, $M = M(x)$ and $R = R(x)$ is described in [14] from which the transfer matrix expression has been obtained:

$$\begin{bmatrix} w(x) \\ \varphi(x) \\ M(x) \\ R(x) \end{bmatrix} = \begin{bmatrix} A_{1,1} & A_{1,2} & A_{1,3} & A_{1,4} \\ A_{2,1} & A_{2,2} & A_{2,3} & A_{2,4} \\ A_{3,1} & A_{3,2} & A_{3,3} & A_{3,4} \\ A_{4,1} & A_{4,2} & A_{4,3} & A_{4,4} \end{bmatrix} \cdot \begin{bmatrix} w_i \\ \varphi_i \\ M_i \\ R_i \end{bmatrix} \quad (12)$$

The kinematical and kinetic variables at node i are denoted by index “ i ” in (12). By setting $x = L$ in (12) the dependence of the nodal variables at node k on the nodal variables at node i will be obtained (see Figure 2).

2.1 Axial free vibration

The equilibrium equation for the axial vibration (according to Figure 1) and the constitutive equation of the FGM beam are:

$$N' = n + (k_x - \mu\omega^2)u \quad (13)$$

$$u' = \frac{N}{EA} + \varepsilon^e \quad (14)$$

Here, n is the axial distributed load; N and N' denote the axial force and its first derivative respectively. The modulus of elastic foundation in the axial direction is $k_x = k_x(x)$; $u = u(x)$ and u' refer to the axial displacement and its first derivative. ε^e is the axial applied strain. $EA = E_L^{NH}(x)A$ is the homogenized beam stiffness in axial direction, and ω is the natural frequency.

By combination of the equations (13) and (14) we get the differential equation

$$\eta_2 u'' + \eta_1 u' + \eta_0 u = n \quad (15)$$

with non-constant polynomial coefficients: $\eta_2 = EA$, $\eta_1 = E'A$, $\eta_0 = \mu\omega^2 - k_x$. In the modal axial vibration analysis the right side of the equation (15) is equal to zero. The solution of the differential equation (15) for $n = 0$ can be expressed by transfer functions \bar{b}_j and has the form:

$$\begin{bmatrix} u(x) \\ u'(x) \end{bmatrix} = \begin{bmatrix} \bar{b}_0 & \bar{b}_1 \\ \bar{b}_0' & \bar{b}_1' \end{bmatrix} \cdot \begin{bmatrix} u_i \\ u_i' \end{bmatrix} \quad (16)$$

The \bar{b}_j - functions ($j \in \langle 0,1 \rangle$) are the solution functions of the differential equation (15). If the $u'(x)$ and $u(x)$ are replaced with the expression (14), we get:

$$\begin{bmatrix} u(x) \\ N(x) \end{bmatrix} = \begin{bmatrix} \bar{b}_0 & \frac{\bar{b}_1}{E_i A_i} \\ EA \bar{b}_0' & \frac{EA}{E_i A_i} \bar{b}_1' \end{bmatrix} \cdot \begin{bmatrix} u_i \\ N_i \end{bmatrix} \quad (17)$$

By setting $x = L$ in (17) the dependence of the nodal variables at node k on the nodal variables at node i will be obtained (see Figure 2). The transfer functions become the transfer

constants which can be calculated by a simple numerical algorithm [17]. E_i is the initial value of the homogenized elasticity modulus $E_L^{NH}(x)$ at node i .

2.1 Finite element matrix derivation

Figure 2 shows two nodal finite element with 6 degrees of freedom.

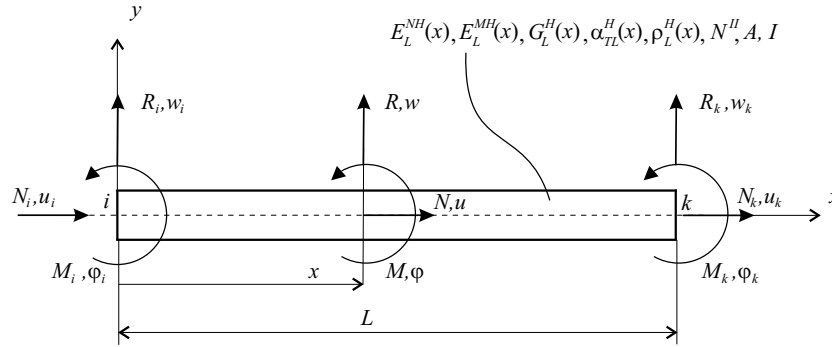


Figure 2: FGM beam finite element

The finite element equation in local coordinate system x, y (18) has been obtained by combination of the equations (12) and (17) and it has a form:

$$\underbrace{\begin{bmatrix} N_i \\ R_i \\ M_i \\ N_k \\ R_k \\ M_k \end{bmatrix}}_{\mathbf{F}_{loc}^e} = \underbrace{\begin{bmatrix} B_{1,1} & 0 & 0 & B_{1,4} & 0 & 0 \\ 0 & B_{2,2} & B_{2,3} & 0 & B_{2,5} & B_{2,6} \\ 0 & B_{3,2} & B_{3,3} & 0 & B_{3,5} & B_{3,6} \\ B_{4,1} & 0 & 0 & B_{4,4} & 0 & 0 \\ 0 & B_{5,2} & B_{5,3} & 0 & B_{5,5} & B_{5,6} \\ 0 & B_{6,2} & B_{6,3} & 0 & B_{6,5} & B_{6,6} \end{bmatrix}}_{\mathbf{B}_{loc}^e} \cdot \underbrace{\begin{bmatrix} u_i \\ w_i \\ \varphi_i \\ u_k \\ w_k \\ \varphi_k \end{bmatrix}}_{\mathbf{U}_{loc}^e} \quad (18)$$

The non-constant terms $B_{i,j}$ (functions of $\omega, N^H, k^{sm}, \bar{k}, k_x$ and other beam parameters) of the symmetric local finite element matrix \mathbf{B}_{loc}^e are not expressed in detail here from space spending point of view. Those are calculated numerically. \mathbf{F}_{loc}^e and \mathbf{U}_{loc}^e is the vector of the local element forces and vector of the local element displacements, respectively.

The global finite element matrix \mathbf{B}_{glob}^e is obtained by usual transformation of the local matrix \mathbf{B}_{loc}^e , $\mathbf{B}_{glob}^e = \mathbf{T}^{eT} \mathbf{B}_{loc}^e \mathbf{T}^e$. \mathbf{T}^e is the well known transformation matrix, \mathbf{T}^{eT} is its transposed form. The global finite element equation reads

$$\mathbf{F}_{glob}^e = \mathbf{B}_{glob}^e \mathbf{U}_{glob}^e \quad (19)$$

where \mathbf{F}_{glob}^e and \mathbf{U}_{glob}^e is the vector of global forces and vector of the global displacements, respectively. Finally, the algebraic system of equations of whole beam structure will be established by a usual way.

The beam structure natural eigenfrequency ω_{ki} (for the calculated thermal forces N'' in the finite element) has been iterative calculated by software MATEMATICA [18]. The natural eigenfrequency ω will be increased until all the boundary conditions have been fulfilled. In this state, the natural frequency ω responds to the i -th natural eigenfrequency ω_{ki} . As the natural eigenfrequency is known, the eigenfrequency and corresponding eigenmode can be calculated by a usual way.

3 NUMERICAL EXPERIMENTS

The actuator (Figure 3) is loaded with thermal load caused by Joule heat. Undeformed and deformed form of the actuator is shown in the Figure 3a. Thermoelastic deformation induces the vertical displacement δ or the action force in the point m . Maximal action force arises when displacements at this point are restrained (Figure 3b). The design of actuator requires not only electro-thermo-structural analysis but also modal analysis. For its performance, mechanical model of beam structure according to Figure 3b have been considered. Three different analyses depending on the type of material have been analysed in order to find its influence on eigenfrequencies of the system. In the first two analyses actuator is the made from one chosen component, in the third one it is made by mixing of two components.

The actuator has been considered as the beam structure (shown in Figure 3b). It consists of 7 parts - beams. Their square cross-section is constant $b = h = 10 \mu\text{m}$. Lengths of the parts are: $L_i = 300 \mu\text{m}$, $i = 1 - 7$. The angles α_1 and α_2 are: $\alpha_1 = 70^\circ$, $\alpha_2 = 20^\circ$.

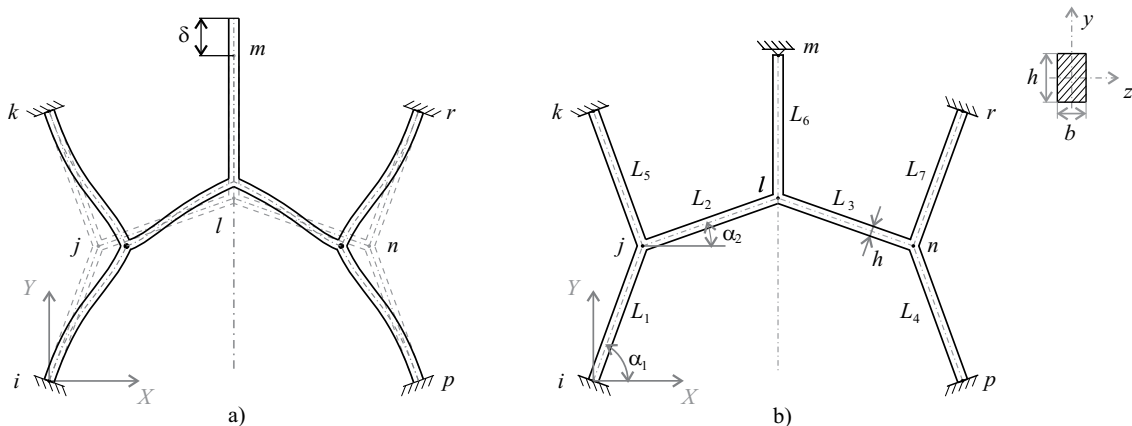


Figure 3: The geometry of the actuator

3.1 Case I – actuator with constant material properties

In this case two analyses have been made. Firstly, the actuator has been made only from aluminum Al6061-TO with constant material properties: the elasticity modulus $E = 69.0 \text{ GPa}$, the mass density $\rho = 2700 \text{ kgm}^{-3}$, the Poisson's ratio $\nu = 0.33$, the coefficient of thermal expansion $\alpha_T = 23.5 \times 10^{-6} \text{ K}^{-1}$. In the next analysis, the actuator has been made from titanium carbide TiC that constant material properties are: the elasticity modulus $E = 480.0 \text{ GPa}$, the mass density $\rho = 4920 \text{ kgm}^{-3}$, the Poisson's ratio $\nu = 0.20$ and the coefficient of thermal expansion $\alpha_T = 5.9 \times 10^{-6} \text{ K}^{-1}$.

The actuator (Figure 3) clamped at the nodes i, k, r, p and simply supported at the node m has been studied by modal analysis. The first three eigenfrequencies have been found (see Table 1) using our new FGM beam finite element. The 1st order beam theory ($N'' = 0$) has been taken into account. Only one our new finite element was used for each part. The same problem has been solved using 10 BEAM3 elements of the FEM program ANSYS [19].

Table 1: Eigenfrequency of the actuator made of one constituent

Eigenfrequency [Hz]	Al6061-TO		TiC	
	New finite element	ANSYS	New finite element	ANSYS
1 st	290682	291325	567956	569214
2 nd	392640	394158	767167	770134
3 rd	395534	397081	772821	775845

As shown in Table 1, the values obtained by both finite elements agree very well with each other.

3.3 Case II – FGM actuator

The FGM actuator with the same geometry as in previous cases has been considered (as shown in Figure 3). Material of the beams consists of two components: aluminum Al6061-TO as a matrix and titanium carbide TiC as a fibre. Material properties of the components are constant (not temperature dependent), same as in previous experiments. There are considering two different longitudinal variation of the fibres volume fraction and have been chosen as the polynomial function of the local beam axis x :

$$a) \quad v_f(x) = 1 - \frac{1}{150}x + \frac{1}{90000}x^2 \qquad b) \quad v_f(x) = \frac{1}{100}x - \frac{1}{30000}x^2$$

that are shown in Figure 4. The first variation of the fibres volume fraction (denoted by a) has been considered in parts 1, 4, 5 and 7 (with initial point i, p, k and r) and the second variation of the fibres volume fraction (denoted by b) in parts 2, 3 and 6 (with initial point j, m, n and). According to Figure 4a-b zero values of the fibres volume fraction at the points j, l and n have been assumed.

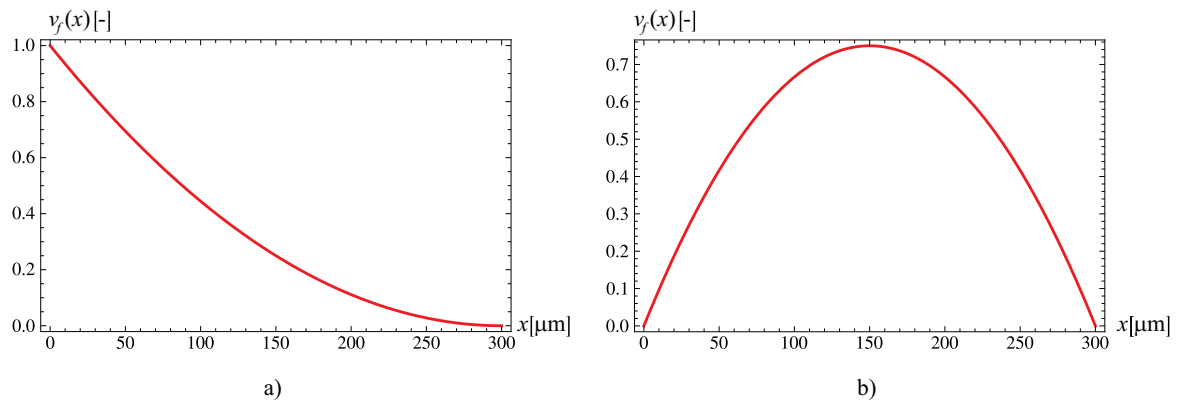


Figure 4: Fibre volume fraction variation

The effective material properties of the homogenized beams (as a function of their local x -axis) have been calculated by the direct integration method [14] and we have got for the first a) variation of the fibres volume fraction (distribution of the elasticity modules are shown in Figure 5a):

$$\begin{aligned}
 E_L^{NH}(x) &= E_L^{MH}(x) = 4.8 \times 10^8 - 2.740 \times 10^{12} x + 4.566667 \times 10^{15} x^2 & [\text{kPa}] \\
 G_L^H(x) &= 1.84615 \times 10^8 - 1.05385 \times 10^{12} x + 1.75641 \times 10^{15} x^2 & [\text{kPa}] \\
 \rho_L^H(x) &= 4920 - 1.48 \times 10^7 x + 2.46667 \times 10^{10} x^3 & [\text{kgm}^{-3}] \\
 \alpha_{TL}^H(x) &= \frac{0.01128 - 0.000072486x + 1.2081 \times 10^{-7} x^2}{480 - 2.74x + 0.004566667x^2} & [\text{K}^{-1}]
 \end{aligned}$$

and for the second b) variation of the fibres volume fraction (distribution of the elasticity modules are shown in Figure 5b)

$$\begin{aligned}
 E_L^{NH}(x) &= E_L^{MH}(x) = 6.9 \times 10^7 + 4.11 \times 10^{12} x - 1.37 \times 10^{16} x^2 & [\text{kPa}] \\
 G_L^H(x) &= 2.65385 \times 10^7 + 1.58077 \times 10^{12} x - 5.26923 \times 10^{15} x^2 & [\text{kPa}] \\
 \rho_L^H(x) &= 2700 + 2.22 \times 10^7 x + 7.4 \times 10^{10} x^3 & [\text{kgm}^{-3}] \\
 \alpha_{TL}^H(x) &= \frac{0.0004071 + 0.000108729x + 3.6243 \times 10^{-7} x^2}{69 + 4.11x - 0.0137x^2} & [\text{K}^{-1}]
 \end{aligned}$$

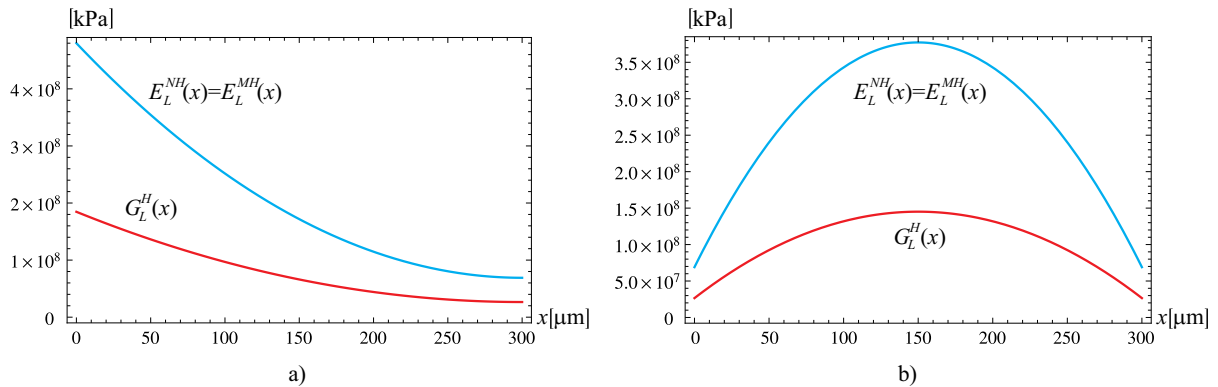


Figure 5: Homogenized elasticity modules

Because of only longitudinal variation of the constituents volume fraction in this case the homogenized elasticity modulus (for axial and transversal loading) are equal each other.

The coefficients of thermal expansion $\alpha_{TL}^H(x)$ were not obtained as a polynomial so expansion to a Taylor series has to be used to convert them into the polynomial form.

The average shear correction factor [15] for all beams is $k^{sm} = 0.83$ (constant Poisson ratio has been assumed for simplicity). The coupled modal analysis of the FGM actuator clamped at the nodes i, k, r, p and simply supported at the node m has been studied. The reference temperature is $T_{ref} = 20^\circ\text{C}$. The thermal forces N^H in the beams and the critical buckling

temperature T_{cr} have been calculated by the BEAM3 finite elements of the FEM program ANSYS [19]. A constant temperature load has been assumed on all parts of the actuator. Thermal axial forces have been evaluated for different temperature $T = 40, 60$ and 80°C and then have been used as input axial forces in the modal analysis. Thermal forces evaluated for different temperature in the actuator are presented in the Table 3. The load temperatures in Table 3 are lower as the critical buckling temperature of the FGM actuator, which is of 128°C . So the pre-buckling thermal loading has been assumed.

Table 3: Thermal forces for different temperature

Thermal forces [μN]	40 °C	60 °C	80 °C
beam 1, 4	-6969	-13940	-20909
beam 2, 3	-4489	-8979	-13469
beam 5, 7	-5331	-10663	-15995
beam 6	-3077	-6155	-9232

The effect of the varying thermal axial force on the actuator eigenfrequency has been evaluated. The first three eigenfrequencies have been found for each set of thermal axial forces (see Table 4) using the new FGM beam finite element for modal analysis. Only one our new finite element was used for each actuator's part. The same problem has been solved using a fine mesh – 1400 of BEAM3 elements (each element has different constant material properties) of the FEM program ANSYS [19]. The average relative difference Δ [%] between eigenfrequencies calculated by our method and the ANSYS solution has been evaluated.

Table 4: Eigenfrequencies of the FGM actuator

Eigen- frequency [Hz]	T = 20 °C ($N^H = 0$)			T = 40 °C			T = 60 °C			T = 80 °C		
	new finite element	ANSYS	Δ [%]									
1 st	471059	472690	0.35	437598	442590	1.13	397697	402240	1.13	347590	350830	0.92
2 nd	595574	592030	0.60	551678	558870	1.29	499444	505190	1.14	436003	440390	1.00
3 rd	610157	604660	0.91	571254	562620	1.58	519027	530010	2.11	498556	493660	1.00

The results, obtained for the thermal loading free state ($T_{ref} = 20, N^H = 0$) which are presented in Table 1 and Table 4, show the effect of mixture of the both components on the eigenfrequency. The eigenfrequencies of FGM actuator lies between the eigenfrequencies of actuator made of only one constituent.

The first three vibration eigenforms for thermal axial forces evaluated for temperature $T = 60\text{ }^{\circ}\text{C}$ are shown in Figure 6.

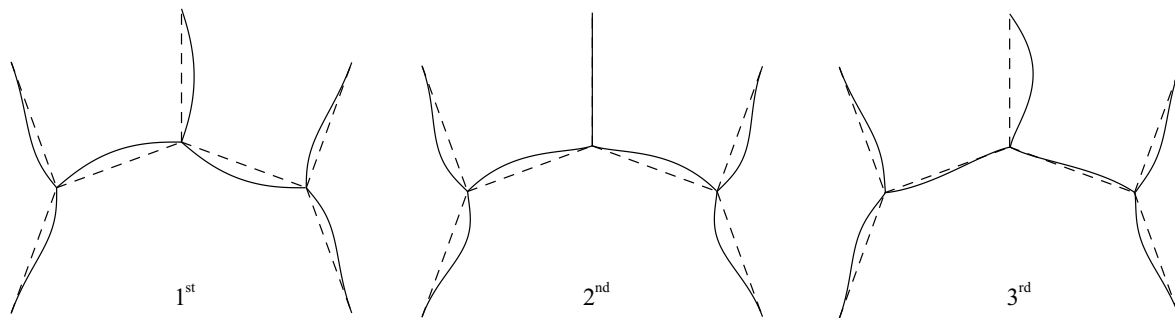


Figure 6: The first three vibration eigenforms: $T=60^{\circ}\text{C}$

The effect of thermal axial forces evaluated for different temperatures (Table 3) on the eigenfrequencies is shown in Figure 7. As expected, the eigenfrequency decreases with increasing thermal load.

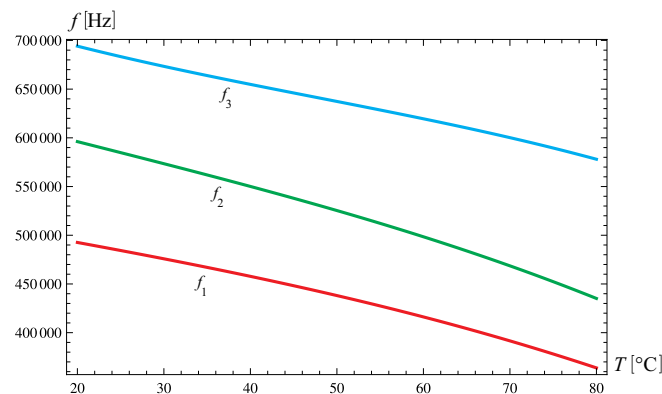


Figure 7: The effect of thermal axial forces evaluated for different temperature on the eigenfrequencies

4 CONCLUSIONS

Modal analysis of chosen actuator which is built of the FGM beams has been done by our new 2D beam finite element. Effects of the material properties and thermal axial forces on the eigenfrequency were analyzed. The temperature loads are lower than the critical buckling temperature.

The obtained results by this new finite element have been studied and compared with results obtained by a fine mesh of the BEAM3 finite element of the program ANSYS. The main additions of our new approach are:

- Eigenfrequency of the actuator is dependent on the operating load, which is caused by internal compressive axial forces in the respective beams;
- Eigenfrequencies of the system can be optimized by functional gradation of its material properties;
- Our new FGM finite element can be used in very efficient modal and buckling analysis of 2D mechatronic beam-like structures.

ACKNOWLEDGEMENT

This paper has been supported by Grant Agency VEGA, project No. 1/0534/12.

This paper has been supported by Grant Agency KEGA, project No. 015STU - 4/2012.

This paper has been supported by APVV 0450 – 10.

This paper has been supported by CRISIS ITMS 26240220060.

REFERENCES

- [1] Zou, H. Zhang, H. Wang, G, Li J. Rapid manufacturing of FGM components by using electromagnetic compressed plasma deposition. Progress in Electromagnetics research symposium proceedings. Moscow, Russia, August 18-21, pp. 1953-1956. (2009).
- [2] Altenbach, H., Altenbach, J., Kissing W. *Mechanics of Composite Structural Elements*, Engineering - Monograph (English). Springer-Verlag, (2003).
- [3] Alshorbagy, A.E., Eltaher, M.A, Mahmoud FF. Free vibration characteristics of a functionally graded beam by finite element. *Applied Mathematical Modelling* 35, pp. 412-425, (2011).
- [4] Lu, C.F., Chen, W.Q., Xu, R.Q. and Lim, C.W. Semi-analytical elasticity solutions for bi-directional functionally graded beams. *Int J Solids Struct* (2008) **45**:258–275.
- [5] Ray, M.C. and Sachade, H.M. Finite element analysis of smart functionally graded plates. *Int J Solids Struct* (2006) **43**: 5468–5484.
- [6] Chakraborty, A., Gopalakrishnan, S. and Reddy, J.N. A new beam finite element for the analysis of functionally graded materials. *Int J Mech Sci* (2003) **45**:519–539
- [7] Arciniega, R.A. and Reddy, J.N. Large deformation analysis of functionally graded shells. *Int J Solids Struct* (2007) **44**:2036–2052,
- [8] Mang, H.A., Eberhardsteiner, J., Bohm, H.J. and Rammerstorner F.G. (ed.) Proceedings of the 6th European Congress on Computational Methods in Applied Sciences and Engineering (ECCOMAS 2012), Vienna, Austria, September 10-14, (2012).
- [9] Pimenta, Paulo M. (ed.) 10th World Congress on Computational Mechanics (WCCM2012). Sao Paulo – Brazil, 8-13 July, (2012).
- [10] Proceedings ECCM15 - 15Th European Conference on Composite Materials, Venice, Italy, 24-28 June (2012).
- [11] Pradham, S.C. and Murmu, T. Thermo-mechanical vibration of FGM sandwich beam under variable elastic foundations using differential quadrature method. *Journal of Sound and Vibration* (2009) **321**:342–362,
- [12] Ke, L.L., Yang, J., Kitipornchai, S. An analytical study on nonlinear vibration of functionally graded carbon reinforced composite beams. *Composite Structures* (2010) **92**:676–683
- [13] Simsek, M. Vibration analysis of a functionally graded beam under a moving mass by using different beam theories. *Composite Structures* (2010) **92**:904–917
- [14] Murin, J., Aminbaghai, M., Kutis, V., Hrabovsky, J. Modal analysis of the FGM beams with effect of axial force under longitudinal variable elastic Winkler foundation. *Engineering Structures* (2013) **49**:234–247,.
- [15] Murin, J., Aminbaghai, M., Hrabovsky, J., Kutis, V., Kugler, S. Modal analysis of the FGM beams with effect of the shear correction function. *Composites: Part B* (2013) **45**:1575–1582
- [16] Murin, J., Aminbaghai, M., Hrabovsky, J., Kutis, V. New FGM beam finite element for modal analysis of the 2D beam structures. *ECCOMAS 2012*, Vienna Austria, September 10–14, (2012).
- [17] Rubin, H., Analytische Berechnung von Stäben und Stabwerken mit stetiger Veränderlichkeit von Querschnitt, elastischer Bettung und Massenbelegung nach Theorie erster und zweiter Ordnung, *Baustatik - Baupraxis 7. Berichte der 7. Fachtagung "Baustatik - Baupraxis"* Aachen/Deutschland 18.-19. März 1999. Balkema 1999, Abb., Tab.S.135-145
- [18] S. Wolfram MATHEMATICA 5, Wolfram research, Inc., 2003.
- [19] ANSYS Swanson Analysis System, Inc., 201 Johnson Road, Houston, PA 15342/1300, USA.